Acta Biomaterialia 6 (2010) 1505–1514

Contents lists available at ScienceDirect

Acta Biomaterialia

journal homepage: www.elsevier.com/locate/actabiomat

Mechanistic aspects of the fracture toughness of elk antler bone

M.E. Launey [a], P.-Y. Chen [b], J. McKittrick [b], R.O. Ritchie [a,c,*]

[a] Materials Sciences Division, Lawrence Berkeley National Laboratory, Berkeley, CA 94720, USA
[b] Materials Science and Engineering Program, Department of Mechanical and Aerospace Engineering, University of California, San Diego, CA 92093, USA
[c] Department of Materials Science and Engineering, University of California, Berkeley, CA 94720, USA

ARTICLE INFO

Article history:
Received 12 September 2009
Received in revised form 5 November 2009
Accepted 17 November 2009
Available online 24 November 2009

Keywords:
Biomaterials
Elk antler
Cortical bone
Fracture toughness
Resistance-curves

ABSTRACT

Bone is an adaptive material that is designed for different functional requirements; indeed, bones have a variety of properties depending on their role in the body. To understand the mechanical response of bone requires the elucidation of its structure–function relationships. Here, we examine the fracture toughness of compact bone of elk antler, which is an extremely fast-growing primary bone designed for a totally different function than human (secondary) bone. We find that antler in the transverse (breaking) orientation is one of the toughest biological materials known. Its resistance to fracture is achieved during crack growth (extrinsically) by a combination of gross crack deflection/twisting and crack bridging via uncracked "ligaments" in the crack wake, both mechanisms activated by microcracking primarily at lamellar boundaries. We present an assessment of the toughening mechanisms acting in antler as compared to human cortical bone, and identify an enhanced role of inelastic deformation in antler which further contributes to its (intrinsic) toughness.

Published by Elsevier Ltd. on behalf of Acta Materialia Inc.

1. Introduction

Biological materials are mostly complex systems in which large numbers of functionally diverse, and frequently multifunctional, sets of elements interact selectively and nonlinearly to produce coherent behavior. One of the most intriguing of these materials is bone, which is a highly hierarchical composite of assemblies of collagenous protein molecules, water, and mineral carbonated hydroxyapatite nanoparticles that form a tough, lightweight, adaptive and multi-functional material. Bone is often stereotyped as a protective and supportive framework for the body; though it performs these functions, it is a dynamic organ that is constantly remodeling and changing shape to adapt to the forces placed upon it. Like all natural materials, its mechanical properties are determined by its structure [1–3], which in turn is defined by its (primarily mechanical) function [4,5]. The adaptation of compact bone to its mechanical environment includes both alteration of its shape and adaptation of its internal structure and hence properties. This dual optimization of form and structure is well known in engineering materials; however, in natural materials both are intimately related due to their common origin, the growth of the organ. Different bones grow at different rates, and the kind of primary bone laid down depends on this rate of accretion. Accordingly, different bones have different mechanical properties [4,5] depending on the growth, structure and adaptation, all of which are interconnected to serve a specific function.

We focus here on the fracture resistance of non-structural[1] bone, namely the compact bone of elk antler. With the exception of reindeers, antlers are found only in males, and are grown in the spring and summer, used in the rut in the fall, and are shed in the winter. Unlike human bone, they provide neither structural support nor protection of organs. The functions of antlers are display and fighting, with no load-bearing role and low stiffness compared to skeletal bone; however, they are designed to undergo high impact loading and large bending moments without fracture.

There have been previous evaluations of the toughness of antler [4–7], although many of these have been inaccurate due to problems of inappropriate measurement technique (e.g., measurements based on the area under a compression stress–strain curve). In particular, single-value linear-elastic fracture parameters based on crack initiation, such as K_{Ic},[2] have been used but

[1] "Non-structural" refers here to the non-supportive role of antler bones, e.g., antlers do not bear any loads nor support organs.

[2] For materials that display linear-elastic constitutive behavior, the fracture toughness, K_{ic} (where i = I, II or III), is the critical value of the stress intensity K for unstable fracture in the presence of a pre-existing crack; under tensile opening conditions (i.e., in mode I) $K = Y\sigma_{app}(\pi a)^{1/2} = K_{Ic}$, where σ_{app} is the applied stress, a is the crack length, and Y is a function (of order unity) of crack size and geometry. Alternatively, the toughness can be expressed as a critical value of the strain-energy release rate, G_c, defined as the rate of change in potential energy per unit increase in crack area.

* Corresponding author. Tel.: +1 510 486 5798; fax: +1 510 643 5792.
E-mail address: roritchie@lbl.gov (R.O. Ritchie).

1742-7061/$ - see front matter Published by Elsevier Ltd. on behalf of Acta Materialia Inc.
doi:10.1016/j.actbio.2009.11.026

such measurements cannot capture, or even represent, the multiple length-scale toughening acting in cortical bone that leads to its characteristic resistance-curve (R-curve[3]) behavior [8–10], where the fracture resistance actually increases with crack extension. Antler bone is no exception. Vashishth et al. [11,12] have reported rising R-curve (K_R, crack-extension resistance) behavior in antlers of red deer, and demonstrated that the superior toughness of antler bone is due to its enhanced ability to form microcracks during deformation and fracture. Although such stress-intensity-based R-curves do provide a means to characterize crack propagation, the underlying assumptions for such K_R calculations are based on linear-elastic fracture mechanics (LEFM), which cannot account for the energy associated with plastic deformation[4] during bone fracture (an especially important phenomenon in antler). Specifically, for such LEFM measurements, the prevailing mode of deformation is assumed to be linear elasticity; accordingly, any region of "plasticity" that may form in the vicinity of the crack tip (i.e., the plastic zone) must be small enough to ignore. This places restrictions on how large a test specimen has to be for "valid" toughness measurements; specifically, that the in-plane specimen dimensions of crack size and uncracked ligament width must be at least an order of magnitude larger than the plastic-zone size (termed "small-scale yielding"); additionally, for geometry- and thickness-independent toughness values, the out-of-plane thickness dimension must be equally larger than the plastic zone (termed "plane strain" conditions). For example for antler bone, a LEFM K_{Ic} value of 10 MPa$\sqrt{}$m [6] would require test specimen dimensions (in terms of crack size, ligament depth and thickness) in excess of 50 mm for a valid linear-elastic K_{Ic} based on current ASTM validity criteria [13]. However, because the thickness of the cortical shell in antler bone is typically ~5–10 mm, appropriate section sizes for LEFM K_{Ic} measurements are not feasible. This means that as the test samples used in previous studies in the most part were too small for any form of linear-elastic K measurement, the distribution of local stresses and displacements near a crack tip (i.e., near the fracture origin) would not be well represented by the K-fields [14] and the resulting K-based toughness values would be highly questionable. Consequently, for materials such as antler that display significant plastic deformation prior to fracture [15], LEFM is simply not an appropriate methodology to measure the fracture toughness.

For these reasons, a preferred, indeed essential, strategy to evaluate the fracture toughness of cortical antler bone is to use nonlinear elastic fracture mechanics. This approach can provide a more realistic description of the crack-tip stress and displacement fields and furthermore is able to additionally capture the contribution to the toughness from the energy consumed in "plastic" deformation prior to and during fracture [16,17].

Accordingly, in this work we utilize J-integral[5] measurements to determine the toughness of elk antler cortical bone using R-curves, in the presence of realistically sized small (<1 mm) cracks, to characterize the toughness associated with both crack initiation and growth.[6] We confirm that antler bone is the toughest hard mineralized tissue reported to date, and provide a description of the toughening mechanisms underlying its exceptional resistance to fracture.

2. Structure and properties of elk *Cervus elaphus canadensis* antler bone

The microstructure of the compact bone of antler is compared in Fig. 1 with that of human humerus. Elk antler is a young bone predominantly composed of primary osteons [20] that contain vascular channels (15–25 μm diameter) surrounded by concentric bone lamellae (Fig. 1a and c). The entire primary osteons are 100–200 μm in diameter. In comparison, human bone is a secondary (replacement) bone that is the product of resorption of previously existing bone tissue and the deposition of new bone in its place. This process results in the formation of secondary osteons[7] that have central vascular channels 50–90 μm in diameter, known as Haversian canals (Fig. 1b and d); these are surrounded by a series of concentric lamellae containing osteocytes arranged in circular fashion. The entire secondary osteons (or secondary Haversian systems) are about 200–300 μm in diameter. In antler bone (Fig. 1c), a prominent hyper-mineralized region surrounding the primary osteons [20] is present, whereas in the human bone (Fig. 1d), a thin mineralized region, the cement line [21], surrounds the secondary osteons. As prominent sites for microcracking, both have strong implications for fracture behavior [22,23].

Although antler has a composition very similar to other mammalian long bones, it is the only primary mammalian bone that is capable of regeneration (shedding and re-growth each year). During antlerogenesis (antler growth), the porous core and the vascular channels are filled with blood, which provides hydration of the bone, along with the naturally occurring water in living bone. Fully grown antlers had been thought to be dead tissue with all fluid removed once the velvet was shed. More recently, blood-filled fallow deer antlers, with living osteocytes and active osteoblasts, have been found 1 h after casting [24].

Antlers exhibit the fastest growth among all natural calcified tissues, growing as much as 14 kg in 6 months, with a peak growth rate of up to 20–40 mm per day [25]. Such physiological effort of growth necessitate a large import of minerals in a short period of time, which in turn results in antlers having the lowest mineral content in the bone family (55–60 wt.%) [5], high collagen content, and consequently low stiffness and yield strength, as compared with human cortical bone (Fig. 2). The organic content, especially the type-I collagen, is also distinctly higher in antler compact bone, resulting in stiffness 2–3 times lower than that of human cortical bone [3]; with an ultimate strength of ~145–160 MPa in the transverse direction [4,6], this confers more extensibility and a higher work to fracture [6] such that it exhibits extensive deformation prior to fracture (a functional adaptation). Indeed, the yield strength of antler compact bone in the transverse direction is as

[3] The crack resistance-curve or R-curve provides an assessment of the fracture toughness in the presence of subcritical crack growth. It involves measurements of the crack-driving force, e.g., K or J, as a function of crack extension (Δa). The value of the driving force at $\Delta a \rightarrow 0$ provides a measure of the crack-initiation toughness, whereas the slope or the maximum value of the R-curve can be used to characterize the crack-growth toughness.

[4] Plastic deformation here is used as a general term to indicate any of the inelastic, non-recoverable deformation mechanisms, such as local collagen fibrillar shearing, viscoplasticity, and microcracking, that are active at various length-scales in bone.

[5] J is the nonlinear strain-energy release rate, i.e., the rate of change in potential energy for a unit increase in crack area in a nonlinear elastic solid. It is the nonlinear elastic equivalent of the strain-energy release rate G. It characterizes the stress and displacement fields at a crack tip in such a solid, and as such can be used to define the onset of fracture there.

[6] We note here that although there has been some controversy of late [18,19] of the efficacy of using J-integral methods to characterize the fracture toughness of bone, the calculation of the value of J at fracture in a bend sample is absolutely identical to that of the well-known traditional measure of the toughness in bone, that of the "work of fracture", i.e., the energy involved in the fracture process (area under the load–displacement curve) divided by twice the area of the fracture surface. The only difference is that specimens used for work of fracture measurements may not contain a pre-crack or notch.

[7] Antlers undergo limited secondary osteon remodeling and consist mainly of primary osteons [20]. Secondary osteon remodeling arises in response to mechanical stress and takes about 2–4 months in human bone [3]. In antlers, secondary osteon remodeling is unlikely to occur since they do not sustain mechanical loads during the growth process and are only used in sporadic combat for 1–2 months before shedding.

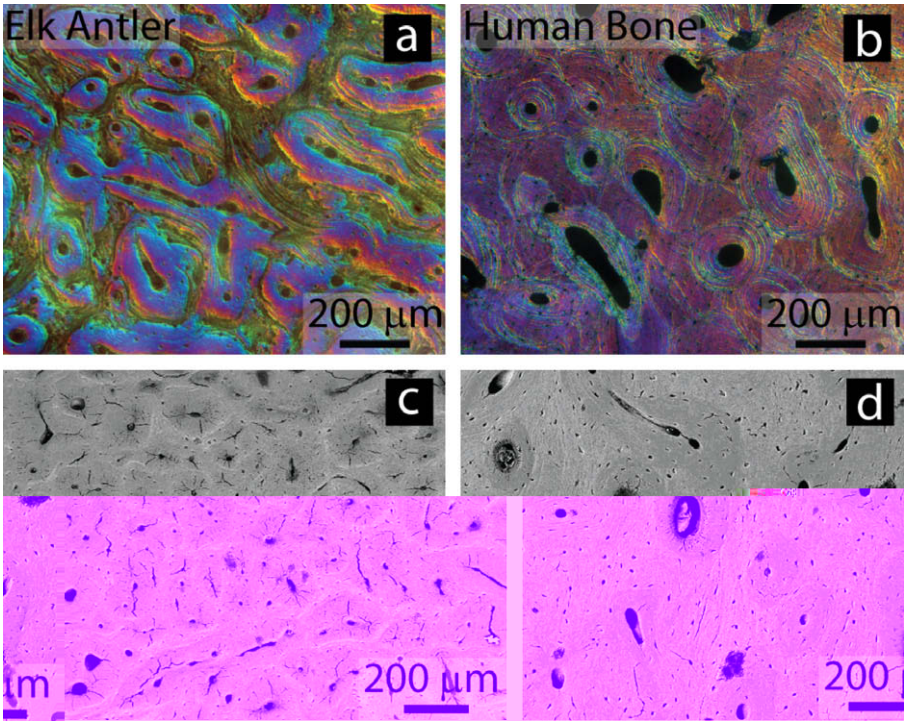

Fig. 1. Microstructure of primary and secondary bone. Differential interference contrast (Nomarski) micrograph of transverse section of compact (cortical) bone of (a) elk antler, and (b) human humerus. (c) and (d) Back-scattered SEM images. Morphologically, the main distinction between primary (c) and secondary bone (d) is that primary osteons do not have cement lines because they are not the product of bone remodeling; however, the interfaces of the primary osteons in antler are thick hyper-mineralized regions. Primary osteons have smaller vascular channels and fewer lamellae than secondary osteons.

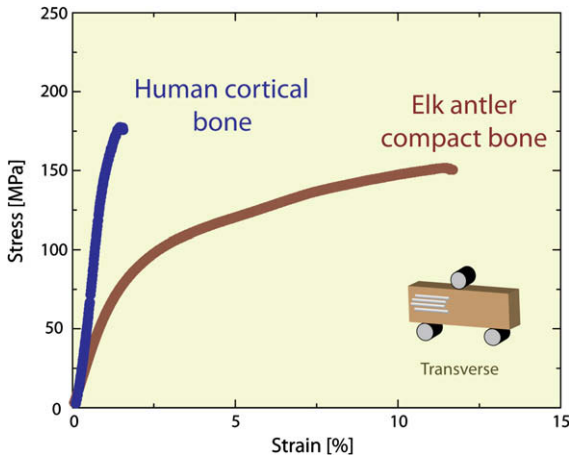

Fig. 2. Stress–strain curves from three-point bending tests for hydrated human cortical bone and elk antler in the transverse orientation. Data for elk antler are taken from Ref. [6].

low as 71 MPa [6], while the corresponding yield strength of human cortical bone is ~110–120 MPa (Fig. 2).

3. Experimental procedures

3.1. Materials

Test samples from the compact region of North American elk (*Cervus elaphus canadensis*) were sectioned using a low-speed saw and machined into eighteen bend samples ($N = 18$). The antler, from a large, mature bull, was shed approximately one year before testing and stored indoors under air-dry condition. Rectangular samples had a thickness B of 2.0–2.2 mm, a width W of 3 mm, and a length of 12 mm. Six samples of each orientations were taken from locations longitudinal or transverse to the bone long axis (Fig. 3a). An initial notch was applied with a low-speed diamond saw and was subsequently sharpened by repeatedly sliding a razor blade over the saw-cut notch, while continually irrigating with 1 μm diamond slurry. The final micro-notches had a root radius of ~3–5 μm. As a result, sharp cracks with initial crack length, $a \approx 1.5$ mm ($a/W \approx 0.5$), were generated in general accordance with ASTM standards [13]. The orientation of the notch was such that the nominal crack-growth direction was either perpendicular to the long axis of the antler (transverse orientation), along the long axis of the antler (in-plane longitudinal), and parallel to the long axis of the antler but perpendicular to the (nominal) crack-propagation direction (anti-plane longitudinal). Each set of samples was further divided into two groups, three to be tested ex situ and three to be tested in situ inside the scanning electron microscope. Prior to testing, all samples were wet polished with an increasingly higher finish to a final polish with a 0.05 μm diamond suspension before being immersed in ambient Hanks' balanced saline solution (HBSS) for 24 h.

3.2. Fracture toughness J–R curve measurements

J–R curves for compact bone of elk antler were performed under rehydrated conditions in mode I (tensile opening) using single-edge notched bend SE(B) specimens with a crack-growth direction (Fig. 3a): (i) transverse to the long axis of the osteons (transverse), (ii) along the direction parallel to the long axis of the osteons (in-plane longitudinal), and (iii) along the direction parallel to the long axis of the osteons but perpendicular to the (nominal) crack-propagation direction (anti-plane longitudinal).

R-curves were measured ex situ in 25 °C HBSS to evaluate the fracture resistance in terms of the J-integral as a function of crack extension, Δa, under a monotonically increasing driving force. Tests were conducted in three-point bending with a span

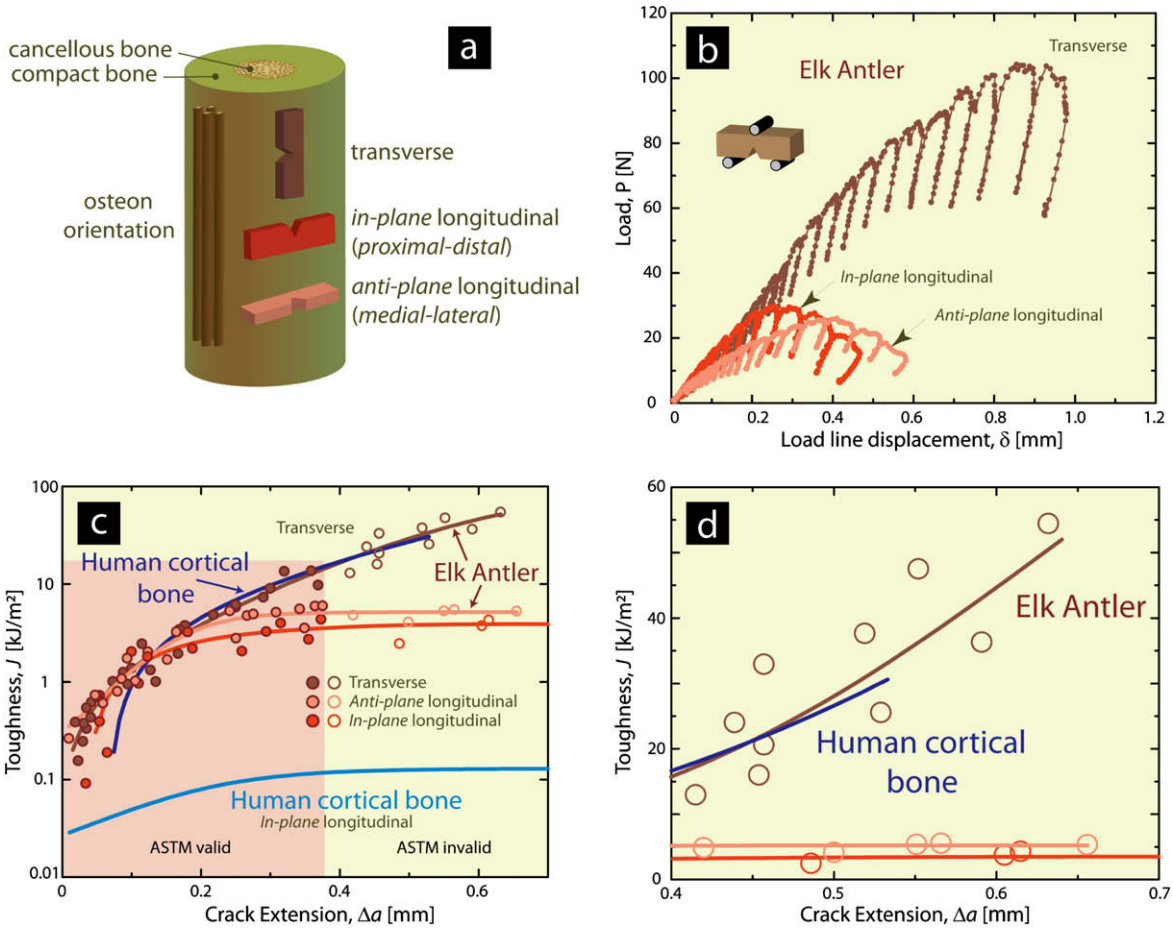

Fig. 3. The schematic (a) shows the structure of antler bone, as well as the three anatomical orientations that the specimens were taken from the compact bone. (b) Typical load vs. load-line displacement curve obtained during R-curve testing for the transverse, in-plane longitudinal, and anti-plane longitudinal orientation of antler compact bone. Each partial unloading event during the test corresponds to a data point in (c). (c) Full $J_R(\Delta a)$ resistance curves for stable ex situ crack extension in hydrated antler compact bone tested in transverse, in-plane longitudinal, and anti-plane longitudinal orientations. (d) Expansion of (c) showing $J_R(\Delta a)$ resistance curves at larger crack extension ($\Delta a > 0.4$ mm). The R-curves for short crack lengths ($\Delta a \approx 0.6$ mm) are compared with data taken from human cortical bone in both transverse and in-plane longitudinal orientations of the humerus. Data for human cortical bone were adapted from Ref. [17]. In the transverse orientation, fracture toughnesses, J, of antler compact bone were recorded at nearly ~60 kJ m^{-2}, almost two times higher than the critical toughness value, J_c, of human cortical bone ($J_c \approx 30$ kJ m^{-2}). The validity of these data points is defined by the measurement capacity of each specimen in accordance with the ASTM standard [13]. The circles in (c) and (d) correspond to data points for antler bone.

($S = 10$ mm) to width ($W = 3$ mm) ratio of ~3, in accordance with ASTM E1820-08 [13]. The specimens were loaded in displacement control in a MTS 810 servo-hydraulic testing machine with a loading rate of ~0.015 mm s^{-1} until the onset of cracking, which was determined by non-linearity in the load–displacement curve (Fig. 3b). To monitor subsequent subcritical crack growth, after this point during loading, the sample was periodically unloaded (by ~10–20% of the peak load) to record the elastic load-line compliance using a LVDT mounted on the load frame. After each increment, the specimens were held for 30 s to allow for crack extension to stabilize, followed by unloading compliance measurement. This process was repeated at regular intervals until the end of the test, at which point the compliance and loading data were analyzed to determine J-integral as a function of Δa. Crack lengths, a, were calculated from the compliance data obtained during the test using compliance expression of a three-point bend specimen at load line [26]:

$$a/W = 0.997 - 3.58U - 1.51U^2 - 110U^3 + 1232U^4 - 4400U^5, \quad (1)$$

where U is a fitting function, written as:

$$U = \frac{1}{\sqrt{FC}+1} \quad (2)$$

Here C is the sample compliance, and F is a calibration factor, taken to be that which gives the best agreement between the initial compliance and crack length at the beginning of the test.

In addition, R-curves were measured on HBSS-saturated specimens in situ in a Hitachi S-4300SE/N environmental scanning electron microscope (ESEM) using a Gatan Microtest three-point bending stage. Crack extension was monitored directly in backscattered electron mode at a pressure of 35 Pa and a 30 kV excitation voltage.

R-curve determination was limited to small-scale bridging conditions, where the size of the zone of crack bridges behind the crack tip remained small compared to the in-plane test specimen dimensions. As noted above, the use of the J-integral as the driving force for crack initiation and growth was employed to capture the contribution from inelastic deformation in the evaluation of toughness. The stress intensity at each measured crack length was calculated by measuring the nonlinear strain-energy release rate, J. The value of J was calculated from the applied load and instantaneous crack length according to ASTM standards [13], and was decomposed into its elastic and plastic contributions:

$$J = J_{el} + J_{pl}. \quad (3)$$

The elastic contribution J_{el} is based on linear-elastic fracture mechanics:

$$J_{el} = \frac{K_I^2}{E}, \quad (4)$$

where K_I is the mode I stress-intensity factor, and E is the Young's modulus. Using the load-line displacements, the plastic component J_{pl} for a stationary crack in bending is given by:

$$J_{pl} = \frac{1.9A_{pl}}{Bb}, \quad (5)$$

where A_{pl} is the plastic area under force vs. displacement curve, b is the uncracked ligament length (W–a). K-based fracture toughness values were back-calculated from the J measurements using the standard J–K equivalence for nominally mode I fracture, specifically that $K_J = (JE)^{1/2}$ with the Young's modulus for antler taken as 7 GPa [6].

3.3. Microstructural characterization

The microstructure of antler was characterized using differential interference contrast (Nomarski) microscopy, and scanning electron microscopy (SEM) in both secondary and back-scattered electron mode. Synchrotron X-ray computed micro-tomography (μXCT) was employed to visualize in three-dimensions the crack path and distribution of micro-damage after R-curve testing. The μXCT evaluation was performed at the Advanced Light Source synchrotron radiation facility at Lawrence Berkeley National Laboratory; the setup is similar to standard tomography procedures [27] in that samples are rotated in a monochromatic X-ray beam and the transmitted X-rays imaged via a scintillator, magnifying lens and a digital camera to give an effective voxel size in the reconstructed three-dimensional image of 4.45 μm. The samples were scanned in absorption mode and the reconstructed images were obtained using a filtered back-projection algorithm. In absorption mode, the gray scale values of the reconstructed image are representative of the absorption coefficient. To maximize the signal to noise ratio, the energy was selected at 15 keV; this optimizes the interaction between the X-rays and the sample. Two-dimensional images were taken every quarter of a degree between 0 and 180 degrees. The data sets were reconstructed using the software Octopus [28] and the three-dimensional visualization was performed using Avizo™ software [29].

4. Results

4.1. Resistance-curve behavior

Full $J_R(\Delta a)$ resistance curves for short crack lengths ($\Delta a <$ 0.6 mm) are shown in Fig. 3c and are compared with previous results [17] on human cortical bone. The R-curve testing of antler was terminated after about 0.6 mm of crack growth as none of the specimens broke in half. The specimens bent into a large bow with central loading point typically deforming about 1 mm. It is apparent that antler exhibits significant rising R-curve behavior indicative of extensive toughening. This is the first time that nonlinear elastic fracture mechanics has been used to evaluate the R-curve behavior in antler; results clearly demonstrate that the material, like human bone, derives most of its resistance to fracture during crack growth, and not during crack initiation. J values reach exceptionally high values of ~60 kJ m^{-2} over the first 0.6 mm of crack extension (Fig. 3d), representing the highest toughness reported for any biological material to date [30]. This is twice the toughness of human cortical bone (humerus) in the same orientation ($J \sim 30$ kJ m^{-2}) [17]. In contrast, antlers tested in their longitudinal orientations (in-plane and anti-plane) are far less tough, but still reach (steady-state) fracture toughnesses of $J_c \sim 4$–5 kJ m^{-2}, i.e., more than an order of magnitude higher than in human cortical bone (to extend a crack ~0.5 mm).

The R-curves can also expressed with a stress-intensity K-based description, termed K_J [17] (Fig. 4), where the comparison with human bone is somewhat different (primarily due to the large difference in elastic moduli). For a range of crack extensions up to ~0.5 mm, peak toughnesses for antler are ~20 MPa$\sqrt{}$m in the transverse orientation, which is similar to human bone [17], and ~4–5 MPa$\sqrt{}$m in the longitudinal orientations, which is 2–3 times higher.

According to active ASTM Standards (derived for metallic materials) [13], the maximum J capacity for a specimen is given by the smaller of $J_{max} = b\sigma_y/10$ or $B\sigma_y/10$; similarly, the maximum crack extension capacity is given by: $\Delta a_{max} = 0.25b$. The $J_R(\Delta a)$ curve is therefore defined as the data in a region bounded by these J_{max} and Δa_{max} limits (see Fig. 3c). The maximum measurement capacity of antler specimens were $J_{max} = 10.5$ kJ m^{-2} (with $b = 1.5$ mm) and $\Delta a_{max} = 0.375$ mm (with $b = 1.5$ mm), as illustrated in Figs. 3c and 4. This criterion yields J-integral values that are slightly above J_{max}, which raises questions about the validity of toughness measurements of soft biological materials that exhibit low yield strengths, such as antler. No such standards exist for biological materials, but we believe that since our J measurements are so close to ASTM validity limits (which by definition are conservative), they have a clear physical meaning as specimen dimensions represent the actual size of the bone.

4.2. Crack-growth observations

The salient sources of toughening in antler were identified by performing additional fracture toughness tests in situ in the environmental scanning electron microscope (ESEM) on rehydrated samples. This technique provides the opportunity to measure quantitatively the R-curve while simultaneously monitoring the evolution of damage mechanisms ahead of the growing crack and the toughening mechanisms that result in its wake; furthermore, how these mechanisms relate to the bone architecture can imaged in real time (Fig. 5). Our results show that, similar to human cortical bone, antler combines many toughening mechanisms operating over a range of dimensions to develop toughness through crack

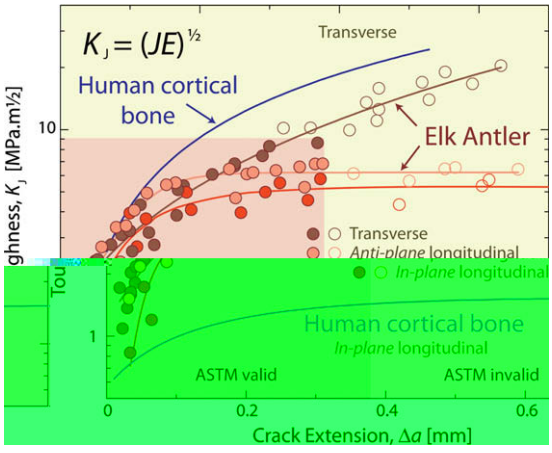

Fig. 4. Crack-resistance curves (R-curves) showing resistance to fracture in terms of the stress intensity, K_J, as a function of crack extension, Δa, for hydrated antler and human compact bone in different orientations. The fracture toughness, K_J, values are back-calculated from the J measurements using the J–K equivalence for mode I fracture. In contrast to Fig. 3c, when compared in terms of K, the transverse toughness of the human cortical bone appears higher because of its 2- to 3-fold higher elastic modulus – $K = (JE)^{1/2}$.

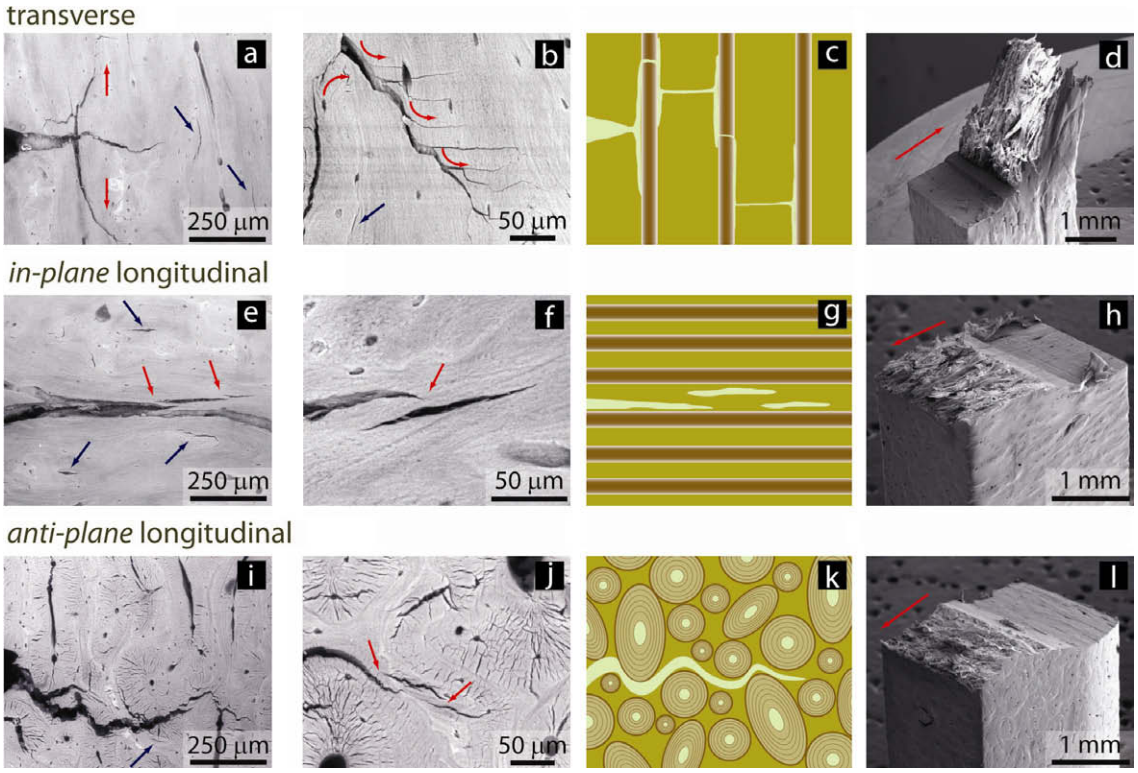

Fig. 5. Mechanisms for stable crack propagation and toughening in the transverse and longitudinal orientations of antler compact bone. ESEM back-scattered electron images of stable crack growth during in situ R-curve testing in the (a and b) transverse, (e and f) in-plane longitudinal, and (i and j) anti-plane longitudinal orientations. (d, h and l) SEM fractography images and (c, g and k) schematics of the crack trajectory for each orientations. In the transverse direction (a–d), the prominent toughening mechanisms are in-plane crack deflection and out-of-plane crack twisting. In the longitudinal orientation (both in-plane and anti-plane), the dominating toughening mechanism is "uncracked-ligament" bridging (e, f and j). The red arrows indicate the direction of deflection in (a), twists in (b), crack propagation in (d, h and l), and uncracked-ligament bridges in (e, f and j) involving two-dimensional uncracked regions along the crack path that can bridge the crack on opening [55]. The blue arrows delineate microcracks that formed at the osteon/matrix interface along the axis of the bone. Such microcracking is essential for many of the toughening mechanisms in bone, notably crack bridging and crack deflection which predominate at micrometer-scales and above.

deflection/twist and crack bridging processes (Fig. 5); both mechanisms result from the occurrence of microcracking [17,31]. Such microcracking is essential for many of the toughening mechanisms in bone, notably crack bridging and crack deflection, which predominate at micrometer-scales and above [32]. In the transverse direction (Fig. 5a–d), the prominent toughening mechanisms are in-plane crack deflection and out-of-plane crack twisting. Mechanistically, the crack deflects by as much as 90 degrees at the interface between the interstitial bone and the osteons (Fig. 5a), and follows it until through-thickness twists occur (Fig. 5b). Three-dimensional μXCT visualizations show such major twists in the transverse (breaking) orientation (Fig. 6c). As microcracking predominates along the "weaker" hyper-mineralized osteon interfaces (and lamellar boundaries), the largest microcracks form along the long axis of the antler. Because this is nominally orthogonal to the fracture direction in the transverse (breaking) orientation, the degree of toughening can be large ($K_{Ic} \sim 20$ MPa$\sqrt{}$m) due to major deflections and twists (Fig. 6b and c) in the crack path as it encounters these "weak" interfaces; resulting fracture surfaces are consequently very rough (Fig. 5a–d).

Conversely, in the longitudinal orientations (both in-plane and anti-plane), the major interfacial microcracks are now nominally parallel to the fracture direction (Fig. 5e). The formation of such microcracks ahead or parallel to the main growing crack leaving intact regions in between; the resulting "uncracked-ligament" bridges [17,31] then carry load that would otherwise be used to further propagate the crack. Crack paths are consequently quite planar with little evidence of deflection (Fig. 6a), resulting in much smoother fracture surfaces. The crack bridges do provide for some degree of toughening ($K_{Ic} \sim 4$–5 MPa$\sqrt{}$m), although it is significantly less than for transverse fractures (Fig. 5e, f and j). In the anti-plane longitudinal orientation, the crack path is deflected around the hyper-mineralized regions (Fig. 5i–k), which additionally contributes to the toughening.

5. Discussion

Although LEFM parameters, such as K_{Ic}, have long been used to estimate the toughness of bone, the approach is only valid where small-scale yielding conditions apply [33], i.e., where the extent of local (crack-tip) inelasticity is small compared to the size of the bone or test sample. Such LEFM methods are thus highly questionable where extensive yielding precedes crack initiation and growth, which is precisely the situation with the fracture of antler bone. Accordingly, to assess the toughness of this material with its large post-yield deformation (Figs. 2 and 3b), a nonlinear elastic fracture mechanics approach is essential. Indeed, such *J*-integral measurements have now been used to quantify the toughness of several biological materials, including bone [16,17,34], dentin [35] and nacre [36].

To appreciate the remarkable toughness of antler and discern the roles of the observed toughening mechanisms, it is noted that the fracture resistance is a multiple-scale process with each level of structural hierarchy adapted to provide optimal toughness. Traditionally, toughness has been thought of as the ability of a material to dissipate deformation energy without propagation of a crack. However, fracture is actually the result of a mutual competition of intrinsic damage mechanisms ahead of the crack tip that

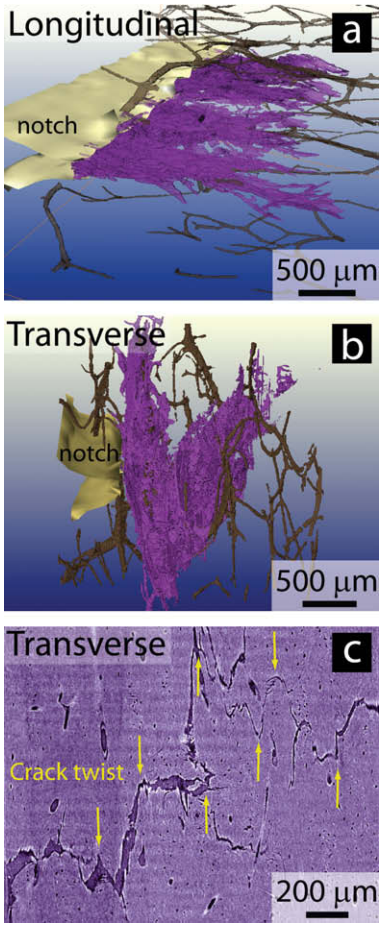

Fig. 6. Synchrotron X-ray computed micro-tomography images of the crack path in both the (a) in-plane longitudinal and (b and c) transverse orientations of antler compact bone. In the longitudinal (splitting) orientation (a), the crack is very planar with little evidence of deflection. In the transverse (breaking) orientation (b), the crack undergoes significant deflection as it interacts with the osteons and lamellar interfaces. (c) A through-thickness slice from the front face to the back face near the crack tip highlighting the twists of the crack through the sample. The arrows indicate some of the major twists at ~90 degrees. Crack paths in the transverse orientation are highly (b) deflected and (c) twisted, resulting in high toughness. The brown lines in (a) and (b) are vascular channels.

promote cracking and extrinsic shielding mechanisms mainly behind the tip that impede it [37,38]. Intrinsic toughening mechanisms increase the microstructural resistance, as exemplified by the role of plasticity ahead of the crack tip in metals. Extrinsic toughening involves microstructural mechanisms that act primarily behind the crack tip to inhibit crack growth by effectively reducing the crack-driving force actually experienced at the crack tip, as shown by crack-tip shielding mechanisms such as crack bridging. We believe that the exceptional toughness of antler is a result of a suite of potent extrinsic (shielding) mechanisms, specifically crack deflection and bridging (Figs. 5 and 6), coupled with an additional role of intrinsic toughening due to the significant "plasticity" in the material (Figs. 2 and 3b).

The antler structure can be viewed as cascaded arrangements of building blocks at defined length scales (subnano to macro) that form a hierarchical structure which controls the properties, i.e., its deformation and toughness [39,40]. Intrinsic toughening, i.e., plasticity, is generated at the nano-level by stretching and unwinding of the collagen, combined with continuous gliding at the micro-scale between tropocollagen molecules and hydroxyapatite particles within the fibrils [41]. The characteristic nanostructure of mineralized collagen fibrils is vital for its high strength and its ability to sustain large deformation, as it is relevant to the physiological role of bone. The staggered arrangement of molecules into fibrils provides its ability to dissipate mechanical energy through molecular sliding rather than leading to catastrophic failure [42,43]; this plays a key part in increasing the toughness of various collagen materials such as tendon or bone [44]. Indeed, it has been reasoned that the dissipation of energy associated with viscoplastic flow with "sacrificial bonding" in the collagen [45,46], and with microcracking, are responsible for the formation of plastic zones around cracks in bone, which is the essence of intrinsic toughening. These nano- and micro-scale "plastic" deformation mechanisms are highly effective in antler; it has the highest strain to failure of the entire bone family, with an ultimate tensile strain of ~12% (Fig. 2), which is six times higher than the ultimate tensile strain of the human cortical bone (~2%) [3]. In fact, the high fracture toughness of antler has traditionally been attributed to the relatively high organic volume fraction and a higher potency of microcracking [11,12,47].

However, from a perspective of fracture resistance, we show in this study that microcracking plays a more critical role at larger length-scales and is in fact essential to the development of the macroscopic toughness from crack bridging and crack deflection [17,31], both of which strongly depend on structure and orientation. Behavior is somewhat similar to human cortical bone where the main structural features that primarily control toughness, the osteons (Figs. 5 and 6), represent a length-scale that is several hundred micrometers in size. In human bone, the major microcracks tend to form at cement lines, and as such are the basis for its orientation-dependent toughness from crack deflection and bridging [17]. Although there are no cement lines in antler, major microcracks form primarily at the hyper-mineralized osteon boundaries and are thus still aligned along the long axis of the bone; during transverse fracture they act as effective local crack arresters (as the Cook–Gordon mechanism [48] in laminates), causing gross crack deflections from the plane of maximum stress (Fig. 5a and d) and correspondingly high toughness. This process of major crack deflections/twists at the osteons is clearly the most potent source of toughening in antler in the transverse orientation. Three-dimensional images of crack propagation in antler reveal extensive (out-of-plane) crack twisting at angles of up to ~90 degrees (Fig. 6c) in addition to in-plane crack deflections (Fig. 6b). Linear-elastic calculations using crack-deflection mechanics [49] show that for in-plane deviations of the crack path, the resulting fracture toughness can be increased by up to a factor of two compared to that for an undeflected crack; where the crack twists out-of-plane, this increase can be significantly higher (factor of six or more) [50].

Although crack deflection/twist is the principal toughening mechanism in the transverse orientation, as noted above, crack bridging also occurs in antler, but unlike in the longitudinal orientation, the bridges are twisted (Fig. 7). We believe that such "twisted bridging" is a further source of toughening in antler. In fracture, crack trajectories result from a competition between the direction of maximum mechanical driving force (maximum G or $K_{II} = 0$) and the path of "weakest" microstructure resistance [51,52]. In contrast to the longitudinal orientations where these preferred mechanical and microstructural crack paths are nominally in the same direction (Fig. 5e–h), these two requirements are incommensurate in the transverse (breaking) orientation, with the maximum driving force oriented parallel and directly ahead of the crack tip (which promotes coplanar cracking), and the "weakest" paths oriented perpendicular to the crack tip along the direction of the major microcracks. With the application of a tensile load promoting crack growth in a direction orthogonal to the path where microstructurally the crack would most like to travel, extensive crack deflection and kinking is inevitable (Fig. 7). This process is repeated several times, before through-thickness crack twisting

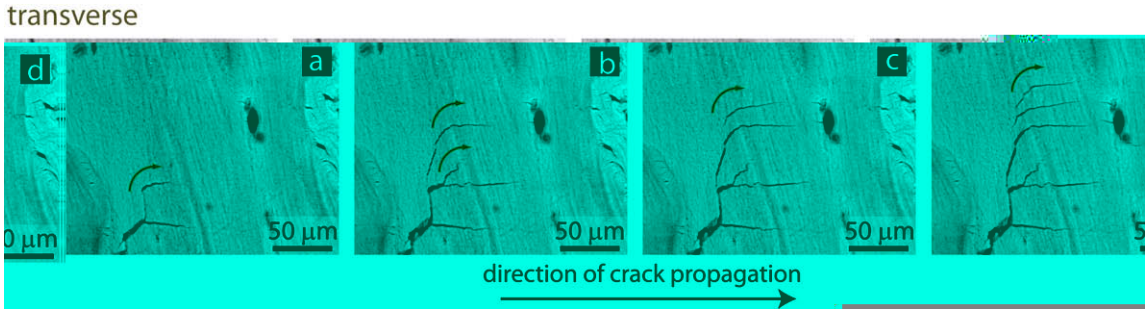

Fig. 7. Toughening mechanism by "twisted bridges". (a–d) Series of ESEM back-scattered electron image taken during in situ R-curve testing in the transverse orientation of antler compact bone after ~300 μm of crack extension and a corresponding toughness J of ~8 kJ m^{-2}. In contrast to the longitudinal orientations where the preferred mechanical and microstructural crack paths are nominally in the same direction (Fig. 4e–h), they are essentially orthogonal for crack advance in the transverse orientation, which leads to the formation of "twisted bridges" and higher toughness. The loading axis is here normal to the general direction of crack propagation along a maximum K_I (or $K_{II} = 0$) path.

occurs at higher applied loads (Fig. 5b), all of which leads to significantly higher toughness in this orientation. Indeed, this mechanism of "twisted bridging" is likely to occur in all bone in the transverse (breaking) orientation; however, to our knowledge, this is the first time that this mechanism has been reported. In the longitudinal orientations, conversely, such preferred mechanical and microstructural crack paths are nominally in the same direction, which results in lower toughness [51].

It is clear that absence of cement lines in antler bone, the refractile boundaries of secondary osteons, does not limit the degree of toughening. In 1875, Von Ebner [53] first described them as "glue lines", yet in human bone they are preferred sites for microcracking (with to a lesser extent the lamellar interfaces), and clearly provide "weak" interfaces to deflect/arrest cracks [23]. As similar microcracking/deflection mechanisms are observed in antler, the hyper-mineralized primary osteon boundaries can clearly also provide this function.

The other characteristic of antler bone is its lower transverse strength and much lower stiffness than human bone, which is associated with its extensive plasticity; this further contributes to its toughness, but now intrinsically. The low yield strength in the longitudinal direction allows crack-tip plastic zones to form at lower stresses than in human bone [11,47], which contributes to the large inelastic deformation and thereby to its intrinsic toughness. Such contributions from nanoscale "plasticity" within the mineralized collagen fibrils are important, although little is known about these mechanisms in antler. Recently, in situ tensile testing on compact antler bone combined with small angle X-ray diffraction measurements [15] revealed that while both antler and (bovine) bone show similar nanoscale fibril shearing mechanisms [42] during elastic deformation, during inelastic deformation, i.e., after macroscopic yielding, they are different with inhomogeneous fibril stretching in antler, leading to defects and consequent debonding between neighboring fibrils. The result is that strain localization in antler is suppressed at the micro-scale; moreover, this process is thought to cause the formation of nano- and microcracks, which further contributes to its extensive inelastic deformation prior to failure.

6. Conclusions

Based on an experimental study of the proper measurement and origins of the exceptional fracture toughness of elk antler bone, the following conclusions can be made:

1. Due to its enhanced elasticity (low stiffness) and "plasticity" (low transverse strength), it is essential to use a nonlinear elastic fracture mechanics approach, e.g., involving J-integral methods, to measure the fracture toughness of antler bone, as linear-elastic analyses fail to capture the toughening contribution from plastic deformation and moreover are simply not valid. Furthermore, as the plastic deformation stabilizes extensive subcritical cracking prior to outright failure, the toughness must be evaluated using crack-resistance curves (R-curves), as this provides an assessment of both the crack-initiation and crack growth toughnesses.
2. Using J-based R-curve measurements for realistic crack extensions below 1 mm, the initiation of cracking was found to occur at less than 1 kJ m^{-2} in all orientations. However, the crack-growth fracture toughness, J_c, of elk antler bone in the transverse (breaking) orientation was found to be as high as ~60 kJ m^{-2}, i.e., twice as high as comparable measurements in human cortical bone.
3. In the longitudinal orientations (in-plane and anti-plane), antler bone was found to be far less tough, reaching (steady-state) fracture toughnesses of $J_c \sim 4$–5 kJ m^{-2}. However, this is more than an order of magnitude higher than comparable measurements to extend a crack some 0.5 mm in human cortical bone. This is due to the more tortuous crack path as it follows the hyper-mineralized regions surrounding the osteons.
4. Similar to human cortical bone, the characteristic rising R-curve behavior of elk antler bone was found to derive from a confluence of toughening mechanisms acting at several length-scales. In addition to an enhanced nano/microcracking capability (as compared to human bone), which promotes inelastic deformation and thereby contributes to its intrinsic toughness (and low strength), antler bone was found to generate significant extrinsic toughening from crack bridging and particularly crack deflection/twist at small crack sizes (<1 mm), both of which resulted from preferential longitudinal microcracking at the hypo-mineralized boundaries of the primary osteons nominally aligned along the long axis of the bone.
5. For loading in the transverse (breaking) orientation, where the direction of the maximum mechanical driving force is essentially orthogonal to the preferred microstructural path along the osteon boundaries, fracture in antler bone is associated with severely (in-plane) deflected and (out-of-plane) twisted crack paths, which results in rough fracture surfaces and very significant extrinsic (crack-growth) toughening.
6. For loading in the longitudinal (splitting) orientations, where the direction of the maximum mechanical driving force is coplanar with the preferred microstructural path, "uncracked-ligament" crack bridges are generated by the formation of microcracks parallel to, and ahead of, the growing crack. Crack paths become quite planar, with little evidence of deflection, and fracture surfaces are relatively smooth. The crack bridging

does provide for some degree of toughening although its effect is significantly less than the crack deflection/twist mechanisms associated with transverse fractures.

7. The observed length scales at each hierarchical level is a result of structural adaptation towards maximizing target materials properties such as strength and toughness. The significance of this is that compared to human bone, antler is tougher yet is not as strong, highlighting the vital distinction between strength and toughness in biological materials [54]. It is this "plasticity" that results in the lower strength of antler, but by the same token this also provides an enhanced intrinsic toughening contribution, which together with the potent extrinsic toughening contributions from crack deflection/twist and crack bridging makes antler bone tougher than human cortical bone and one of the toughest biological materials known.

Acknowledgements

This work was supported by the Director, Office of Science, Office of Basic Energy Sciences, Division of Materials Sciences and Engineering, of the US Department of Energy under Contract No. DE-AC02-05CH11231 (specifically for MEL and ROR). PYC and JM acknowledge financial support from the National Science Foundation Grant DMR 0510138 and the Army Research Office Grant W911-08-1-0461. The X-ray micro-tomography was performed at the Advanced Light Source synchrotron radiation facility (beamline 8.3.2) at the Lawrence Berkeley National Laboratory under the same contract. The authors thank Holly D. Barth for help with the X-ray computed tomographs.

Appendix A. Figures with essential colour discrimination

Certain figures in this article, particularly Figures 2, 4 and 7 are difficult to interpret in black and white. The full colour images can be found in the on-line version, at doi: 10.1016/j.actbio.2009.11.026.

References

[1] Meyers MA, Chen PY, Lin AYM, Seki Y. Biological materials: structure and mechanical properties. Prog Mater Sci 2008;53:1.
[2] Fratzl P, Weinkamer R. Nature's hierarchical materials. Prog Mater Sci 2007;52:1263.
[3] Currey JD. Bones. Princeton: Princeton University Press; 2002.
[4] Currey JD. Mechanical properties of bone tissues with greatly different functions. J Biomech 1979;12:313.
[5] Currey JD. The design of mineralised hard tissues for their mechanical functions. J Exp Biol 1999;202:3285.
[6] Chen PY, Stokes AG, McKittrick J. Comparison of the structure and mechanical properties of bovine femur bone and antler of the North American elk (*Cervus elaphus canadensis*). Acta Biomater 2009;5:693.
[7] Landete-Castilleijos T, Currey JD, Estevez JA, Gaspar-Lopez E, Garcia A, Gallego L. Influence of physiological effort of growth and chemical composition on antler bone mechanical properties. Bone 2007;41:794.
[8] Nalla RK, Kruzic JJ, Kinney JH, Ritchie RO. Mechanistic aspects of fracture and R-curve behavior in human cortical bone. Biomaterials 2005;26:217.
[9] Vashishth D, Behiri JC, Bonfield W. Crack growth resistance in cortical bone: concept of microcrack toughening. J Biomech 1997;30:763.
[10] Malik CL, Stover SM, Martin RB, Gibeling JC. Equine cortical bone exhibits rising R-curve fracture mechanics. J Biomech 2003;36:191.
[11] Vashishth D, Tanner KE, Bonfield W. Experimental validation of a microcracking-based toughening mechanism for cortical bone. J Biomech 2003;36:121.
[12] Vashishth D. Rising crack-growth-resistance behavior in cortical bone: implications for toughness measurements. J Biomech 2004;37:943.
[13] ASTM E1820-08. Annual Book of ASTM Standards, Vol. 03.01: Metals – Mechanical testing; Elevated and low-temperature tests; Metallography. West Conshohocken, Pennsylvania, USA: ASTM International, 2008.
[14] Grellmann W. New developments in toughness evaluation of polymers and compounds by fracture mechanics. In: Grellmann W, Seidler S, editors. Deformation and fracture behaviour of polymers. New York, NY: Springer-Verlag; 2001. p. 3.
[15] Krauss S, Fratzl P, Seto J, Currey JD, Estevez JA, Funari SS, et al. Inhomogeneous fibril stretching in antler starts after macroscopic yielding: indication for a nanoscale toughening mechanism. Bone 2009;44:1105.
[16] Yan JH, Mecholsky JJ, Clifton KB. How tough is bone? Application of elastic–plastic fracture mechanics to bone. Bone 2007;40:479.
[17] Koester KJ, Ager JW, Ritchie RO. The true toughness of human cortical bone measured with realistically short cracks. Nat Mater 2008;7:672.
[18] Vashishth D. Small animal bone biomechanics. Bone 2008;43:794.
[19] Zioupos P, Currey JD. Changes in the stiffness, strength, and toughness of human cortical bone with age. Bone 1998;22:57.
[20] Skedros JG, Durand P, Bloebaum RD. Hypermineralized peripheral lamellae in primary osteons of deer antler: potential functional analogs of cement lines in mammalian secondary bone. J Bone Miner Res 1995;10:S441.
[21] Skedros JG, Holmes JL, Vajda EG, Bloebaum RD. Cement lines of secondary osteons in human bone are not mineral-deficient: new data in a historical perspective. Anat Rec A 2005;286A:781.
[22] Burr DB, Schaffler MB, Frederickson RG. Composition of the cement line and its possible mechanical role as a local interface inhuman compact-bone. J Biomech 1988;21:939.
[23] Yeni YN, Norman TL. Calculation of porosity and osteonal cement line effects on the effective fracture toughness of cortical bone in longitudinal crack growth. J Biomed Mater Res 2000;51:504.
[24] Rolf HJ, Enderle A. Hard fallow deer antler: a living bone till antler casting? Anat Rec 1999;255:69.
[25] Goss RJ. Deer antlers: regeneration, function and evolution. New York, NY: Academic Press; 1983.
[26] Haggag FM, Underwood JH. Compliance of a 3-point bend specimen at load-line. Int J Fract 1984;26:R63.
[27] Kinney JH, Nichols MC. X-ray tomographic microscopy using synchrotron radiation. Annu Rev Mater Sci 1992;22:121.
[28] Vlassenbroeck J, Dierick M, Masschaele B, Cnudde V, Hoorebeke L, Jacobs P. Software tools for quantification of X-ray microtomography. Nucl Instrum Methods Phys Res Sect A 2007;580:442.
[29] Mercury CS. Avizo™ 5.0 3D Visualization Framework. Chelmsford, MA; 2008.
[30] Wegst UGK, Ashby MF. The mechanical efficiency of natural materials. Philos Mag 2004;84:2167.
[31] Nalla RK, Kinney JH, Ritchie RO. Mechanistic fracture criteria for the failure of human cortical bone. Nat Mater 2003;2:164.
[32] Ritchie RO, Buehler MJ, Hansma PK. Plasticity and toughness in bone. Phys Today 2009;62:41.
[33] Knott JF. Fundamentals of fracture mechanics. London, UK: Butterworths; 1973.
[34] Peterlik H, Roschger P, Klaushofer K, Fratzl P. From brittle to ductile fracture of bone. Nat Mater 2006;5:52.
[35] Yan JH, Taskonak B, Platt JA, Mecholsky JJ. Evaluation of fracture toughness of human dentin using elastic–plastic fracture mechanics. J Biomech 2008;41:1253.
[36] Barthelat F, Espinosa HD. An experimental investigation of deformation and fracture of nacre-mother of pearl. Exp Mech 2007;47:311.
[37] Ritchie RO. Mechanisms of fatigue crack-propagation in metals, ceramics and composites: role of crack tip shielding. Mater Sci Eng A 1988;103:15.
[38] Launey ME, Ritchie RO. On the fracture toughness of advanced materials. Adv Mater 2009;21:2103.
[39] Weiner S, Wagner HD. The material bone: structure mechanical function relations. Annu Rev Mater Sci 1998;28:271.
[40] Rho JY, Kuhn-Spearing L, Zioupos P. Mechanical properties and the hierarchical structure of bone. Med Eng Phys 1998;20:92.
[41] Buehler MJ. Molecular nanomechanics of nascent bone: fibrillar toughening by mineralization. Nanotechnology 2007:18.
[42] Gupta HS, Seto J, Wagermaier W, Zaslansky P, Boesecke P, Fratzl P. Cooperative deformation of mineral and collagen in bone at the nanoscale. Proc Natl Acad Sci USA 2006;103:17741.
[43] Buehler MJ. Nature designs tough collagen: explaining the nanostructure of collagen fibrils. Proc Natl Acad Sci USA 2006;103:12285.
[44] Buehler MJ, Yung YC. Deformation and failure of protein materials in physiologically extreme conditions and disease. Nat Mater 2009;8:175.
[45] Thompson JB, Kindt JH, Drake B, Hansma HG, Morse DE, Hansma PK. Bone indentation recovery time correlates with bond reforming time. Nature 2001;414:773.
[46] Fantner GE, Hassenkam T, Kindt JH, Weaver JC, Birkedal H, Pechenik L, et al. Sacrificial bonds and hidden length dissipate energy as mineralized fibrils separate during bone fracture. Nat Mater 2005;4:612.
[47] Zioupos P, Currey JD, Sedman AJ. An examination of the micromechanics of failure of bone and antler by acoustic emission tests and laser scanning confocal microscopy. Med Eng Phys 1994;16:203.
[48] Cook J, Evans CC, Gordon JE, Marsh DM. Mechanism for control of crack propagation and all-brittle systems. Proc R Soc London Ser A 1964;282:508.
[49] Cotterell B, Rice JR. Slightly curved or kinked cracks. Int J Fract 1980;16:155.
[50] Faber KT, Evans AG. Crack deflection processes I: Theory. Acta Metall 1983;31:565.
[51] Ritchie RO, Cannon RM, Dalgleish BJ, Dauskardt RH, McNaney JM. Mechanics and mechanisms of crack-growth at or near ceramic–metal interfaces:

interface engineering strategies for promoting toughness. Mater Sci Eng A 1993;166:221.
[52] Zimmermann EA, Launey ME, Barth HB, Ritchie RO. Mixed-mode fracture of human cortical bone. Biomaterials 2009;30:5877.
[53] Von Ebner V. Uber den feineren bau der knochensubstanz. Sitzungsberichte Deutsch Akad Wissenschaften Berlin 1875;72:49.
[54] Ritchie RO, Koester KJ, Ionova S, Yao W, Lane NE, Ager JW. Measurement of the toughness of bone: a tutorial with special reference to small animal studies. Bone 2008;43:798.
[55] Yang QD, Cox BN, Nalla RK, Ritchie RO. Re-evaluating the toughness of human cortical bone. Bone 2006;38:878.